

Layer-by-layer assembly of colloidal particles deposited onto the polymer-grafted elastic substrate

Kang Chen and Yu-qiang Ma*

National Laboratory of Solid State Microstructures, Nanjing University, Nanjing 210093, China

We demonstrate a novel route of spatially organizing the colloid arrangements on the polymer-grafted substrate by use of self-consistent field and density functional theories. We find that grafting of polymers onto a substrate can effectively control spatial dispersions of deposited colloids as a result of the balance between colloidal settling force and entropically elastic force of brushes, and colloids can form unexpected ordered structures on a grafting substrate. The depositing process of colloidal particles onto the elastic “soft” substrate includes two steps: brush-mediated one-dimensional arrangement of colloidal crystals and controlled layer-by-layer growth driven entropically by non-adsorbing polymer solvent with increasing the particles. The result indicates a possibility for the production of highly ordered and defect-free structures by simply using the grafted substrate instead of periodically patterned templates, under appropriate selection of colloidal size, effective depositing potential, and brush coverage density.

Colloidal particles can self-assemble into a rich variety of highly ordered structures[1] on periodically patterned substrate [2], block copolymer scaffolds [3], vesicle surfaces with the opposite charge [4], and at brush/air interfaces [5, 6] and liquid/liquid [7] or water/air [8] interfaces. The major challenges in this field are how to assemble monodispersed colloids into highly ordered structures with well-controlled sizes and shapes, and how to achieve layer-by-layer growth of ordered structures. Sedimentation is a simplest approach for colloidal crystallization, however, usually leads to uniform or simple close-packed arrays of colloidal particles on smooth substrates. Effective control over interaction and arrangement of colloids[6, 9] is possible by using densely polymer-grafted substrates[10], since the entropically elastic energy of brushes is comparable to thermal energy, and self-assembly depends critically on thermal energy [4]. A balance between depositing force of colloids and entropic force of brushes probably leads to the formation of ordered colloidal crystal structures, rather than highly disordered aggregates.

The grafting of polymers to surfaces is a simple and useful approach to stabilize colloids against aggregation and adsorption. It was experimentally reported [11] that the thickness of brushes can be adjusted between several nm and $1\ \mu\text{m}$. The grafted polymer always exerts a repulsive entropic force on incoming particles, and past works focused on the interaction between polymer brushes and individual incoming particles and how to prevent the adsorption of colloids such as proteins onto surfaces under various grafting density, chain length, and interactions between chains and surface[10]. To the best of our knowledge, there have been no systematic theoretical studies into the self-assembling structures of colloidal particles when deposited onto the grafting substrate. Here, we undertake the first theoretical study of deposition of col-

loidal particles from polymer solvent onto the grafted substrate, and address an important issue about how to realize the spatial organizing dispersions of colloidal particles.

We consider a mixture of n_β solvent chains and n_p colloidal particles with the radius R , in contact with a substrate grafted with n_α polymer chains. The substrate is horizontally placed in xy -plane which is positioned at $z = 0$, and all polymer chains and colloids are allowed in the region $0 \leq z \leq Z_{max}$. Z_{max} is large enough to avoid the influence of brushes and particles, namely the solvent chains attain their bulk property for large values of z [12]. It is shown that aggregates on the deformed polymer brush are anisotropic, and extend along only one direction for minimizing the entropy loss of brush chain conformations[6]. Here, the existence of “settling” force helps to form horizontally oriented cylinders. Thus we assume translational invariance along y for the sake of simplicity, and the calculation can be reduced to the xz plane. The volume of the system V is $L_x \times Z_{max}$, where L_x is the lateral length of the surfaces along the x axes. The grafting density is defined as $\sigma = n_\alpha/L_x$. All polymer chains are of the same polymerization index N and flexible with the same statistical length a , and incompressible with a segment volume ρ_0^{-1} . The probability distribution for molecular conformations of a Gaussian chain α is assumed to take the Wiener form $P[\mathbf{r}_\alpha(s)] \propto \exp[-\frac{3}{2a^2} \int_0^N ds |\frac{d\mathbf{r}_\alpha(s)}{ds}|^2]$, where $\mathbf{r}_\alpha(s)$ denotes the position of segment s on chain α . Recently, Balazs and co-authors [13] have successfully combined a self-consistent field (SCF) theory with a density functional theory (DFT) to study mixtures of diblock copolymer and nanoparticles. Here, we use the grand canonical form of SCF theory which has been proven to be powerful in calculating equilibrium morphologies in polymeric system [12, 13, 14, 15], to deal with polymer solvent and brushes, while particles are treated by DFT [16, 17] to determine their favorite distributions. The grand canonical partition function [12] for the system can be written as $Z_\mu = \sum_{n_\beta=0}^{\infty} e^{n_\beta N \mu} Z_{n_\alpha, n_\beta, n_p}$, where μ is the chemical

*Author to whom correspondence should be addressed. Electronic mail: myqiang@nju.edu.cn.

potential per solvent segment and $Z_{n_\alpha, n_\beta, n_p}$ is the canonical partition function for n_α grafted chains, n_β solvent polymers, and n_p particles:

$$Z_{n_\alpha, n_\beta, n_p} = \frac{1}{n_\beta!} \frac{1}{n_p!} \int \prod_{\alpha=1}^{n_\alpha} D\mathbf{r}_\alpha(s) P[\mathbf{r}_\alpha(s)] \prod_{\beta=1}^{n_\beta} D\mathbf{r}_\beta(s) P[\mathbf{r}_\beta(s)] \prod_{p=1}^{n_p} d\mathbf{R}_p \delta[1 - \hat{\varphi} - \hat{\varphi}_s - \hat{\varphi}_p] \exp\left[-\frac{\nu}{k_B T}\right] \prod_{\alpha=1}^{n_\alpha} \delta(\mathbf{r}_\alpha(0) - \mathbf{r}^\alpha), \quad (1)$$

where the first δ function enforces incompressibility and the second δ function determines the position of the uniformly anchored chain end. k_B is Boltzmann's constant, T is the temperature, and ν is the interaction energy. \mathbf{R}_p is the position of the center of the p th particle. The operators $\hat{\varphi}$, $\hat{\varphi}_s$, and $\hat{\varphi}_p$ represent the local concentrations of grafted chains, solvent, and colloidal particles, respectively. The SCF theory gives the free energy F

$$\frac{NF}{\rho_0 k_B T V} = -\phi \left(\frac{1}{n_\alpha} \sum_{\alpha=1}^{n_\alpha} \ln Q_\alpha \right) - \frac{N}{\rho_0 V} e^{N\mu} Q_s - \frac{N\phi_p}{\rho_0 \pi R^2} \ln \frac{Q_p}{V\phi_p} + \frac{N\nu}{\rho_0 k_B T V} - \frac{1}{V} \int d\mathbf{r} [\xi(1 - \varphi - \varphi_s - \varphi_p) + w\varphi + w_s\varphi_s + w_p\rho_p - \rho_p\Psi(\bar{\varphi}_p)] \quad (2)$$

where φ , φ_s , and φ_p are the local volume fractions of brushes, solvent chains, and particles, and the overall volume fractions of brushes and particles are given by ϕ and ϕ_p . ρ_p stands for the particle center distribution, and the local particle volume fraction is then given by $\varphi_p(\mathbf{r}) = \frac{\rho_0}{N} \int_{|\mathbf{r}'| < R} d\mathbf{r}' \rho_p(\mathbf{r} + \mathbf{r}')$ [13]. $Q_\alpha = \int d\mathbf{r} q_\alpha(\mathbf{r}, s) q_\alpha^\dagger(\mathbf{r}, s)$ represents the single chain partition function of brushes subject to the field w , and $Q_s = \int d\mathbf{r} q_s(\mathbf{r}, s) q_s(\mathbf{r}, 1-s)$ and $Q_p = \int d\mathbf{r} \exp[-w_p(\mathbf{r})]$ are the partition functions for solvent and particles under fields w_s and w_p , respectively. The end-segment distribution functions $q_i(\mathbf{r}, s)$ and $q_i^\dagger(\mathbf{r}, s)$ represent the probability of finding the s^{th} segment at position \mathbf{r} respectively from two distinct ends of chains. q_i satisfies a modified diffusion equation $\frac{\partial q_i}{\partial s} = \frac{a^2}{6} \nabla^2 q_i - w_i(\mathbf{r})q_i$, and q_i^\dagger meets the same diffusion equation but with the right-hand side multiplied by -1 . The last term in Eq.(2) is DFT term [16] accounting for the steric interaction between particles, and the excess free energy $\Psi(\bar{\varphi}_p)$ per particle is from the Carnahan-Starling function [17] with the weighted particle density, $\bar{\varphi}_p(\mathbf{r})$ [13]. The interaction energy ν is given by $N\nu/\rho_0 k_B T = \int d\mathbf{r} [\chi_{bs}N\varphi\varphi_s + \chi_{bp}N\varphi\varphi_p + \chi_{sp}N\varphi_s\varphi_p + g_e z\varphi_p]$, where the χ 's are the Flory-Huggins interaction parameters between the different chemical species. We fix $N = 100$, $\chi_{bs}N = 0$, and $\chi_{bp}N = \chi_{sp}N = 12.0$, since we assume that all the polymers have the same chemical nature, while the particles are insoluble to polymers[18]. In addition, a depositing force is applied normal to the sub-

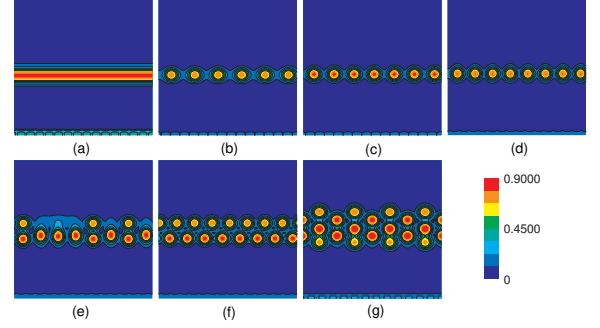


FIG. 1: Particles density distributions in x - z cross-sections under different particle volume fractions. (a) $\phi_p = 0.03$, (b) $\phi_p = 0.04$, (c) $\phi_p = 0.05$, (d) $\phi_p = 0.06$, (e) $\phi_p = 0.092$, (f) $\phi_p = 0.1$, and (g) $\phi_p = 0.145$. The color scale bar shows the local density values of particles in Figs. 1(a)-1(g).

strate, and $g_e > 0$ is the strength of settling field acting on particles. Here, we choose g_e within the range $0.1 \sim 0.6$ which, on one hand, can ensure that the size of particles ($2R = 0.5R_0$) is comparable to the sedimentation length ($\propto \frac{N}{\pi R^2 g_e}$ [19]), $0.8R_0 \sim 5.0R_0$, where $R_0 \equiv aN^{1/2}$ characterizes the natural size of polymer. And on the other hand, the competition between depositing energy of colloids and elastic entropy of deformed brushes can significantly appear within this range of g_e . The volume fraction ϕ_p of particles changes from 0.03 to 0.15 for ensuring the possibility of colloidal crystallization on the brush surface and layer-by-layer growth of colloids. For sub-micrometer particles, the depositing force may be introduced either by gravity or by centrifuge[19, 20], whereas for nano-sized colloids, the sedimentation may be controlled via electrophoretic techniques [20, 21, 22]. We take $\sigma = 0.25$ so that particles hardly embed into the dense brush. A periodical boundary condition for the x -direction is applied, while for the z -direction, the region of $z < 0$ is forbidden and the region $z > Z_{max}$ is treated as a bath of solvent. Z_{max} is fixed to be $60a$, and the lateral length L_x is selected to minimize the free energy of system [23]. All the sizes are in units of a . In SCF theory, the fields and densities are determined by locating saddle points in the free energy subject to the incompressibility: $\varphi(\mathbf{r}) + \varphi_s(\mathbf{r}) + \varphi_p(\mathbf{r}) = 1$. The resulting SCF equations are solved by the combinatorial screening algorithm of Drolet and Fredrickson [15].

We first examine the effects of colloid volume fraction ϕ_p on colloidal dispersions at the top of brushes. Figure 1 shows the morphology changes of dispersed particles with increasing ϕ_p for the parameter $g_e = 0.5$. We find that at low particle volume fraction (Fig.1(a)), the dispersion of particles forms a laterally uniform layer on the top of brushes. This means that the deposition of particles does not deform brushes to in turn react with the dispersion of particles, and particles only spread over the grafting surface, which is similar to that of particles depositing onto

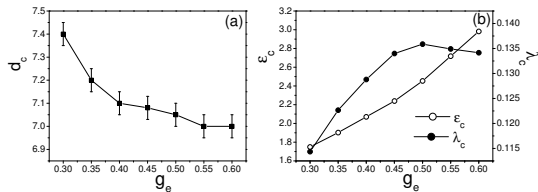


FIG. 2: (a) The minimum spacing d_c between cylinders vs g_e with error bars. (b) The critical correlation factor λ_c and penetration depth ϵ_c as a function of g_e .

the smooth substrate. As more colloidal particles are deposited, the grafted polymer is compressed under depositing potential, and it responds with a restoring force which further drives particles to self-assemble into certain structures for counteracting deposition of particles, in the requirement of minimizing combinational contribution of colloidal depositing energy and brush entropy. Therefore, colloidal particles assemble into colloidal crystals under sedimentation, and morphology of regularly separated cylinder structures emerges. The number of cylinders will increase with the volume fraction ϕ_p (Figs. 1(b)-1(d)). However, further increase of ϕ_p leads to the formation of second layer of cylinders(Figs. 1(e) and 1(f)) piled on the first layer created by brushes, and even forms the third layer of cylinder structures(Fig.1(g)).

The first-layered colloidal structure is formed, due to the competition between colloidal sedimentation and brush entropy effects. For a fixed g_e , the deposited number of cylinders of radius R increases with increasing ϕ_p when the variation of depositing potential per cylinder $g_e \epsilon \pi R^2 k_B T / N \geq \Delta F_b$. Here, ΔF_b represents a brush stretching energy penalty of a local single cylinder with the penetration depth ϵ into the brush [24], which is given by $\Delta F_b = \frac{1}{2} \eta \epsilon^2 \pi$ [25]. For melt brush, the shear modulus $\eta = \eta_0 = 3\sigma^2 k_B T$. We introduce a modified factor λ (i.e., $\eta = \lambda \eta_0$) to account for the correlation effect due to the interplay between multi-cylinders mediated by brushes. Therefore, the variation of λ will mainly depend on the distance d between cylinders. However, we should point out that here, the density profiles of free ends of brushes are diffusive due to the existence of solvent chains above brushes. This will lead to the great decrease of shear modulus compared to that of melt brushes. We have $\lambda \leq \frac{2g_e R^2}{3N\sigma^2 \epsilon}$, and the equality is valid at the critical ϕ_p where the minimum spacing between cylinders is reached, and larger ϕ_p will lead to second-layer aggregation of particles. From the SCFT/DFT calculations, we determine the minimum spacing d_c (Fig. 2(a)) and the critical penetration depth ϵ_c of cylinders(Fig. 2(b)), and find that d_c decreases, whereas ϵ_c increases with g_e . This clearly shows that with increasing g_e , depositing potential of particles is balanced by further deformation of brushes. Figure 2(b) also gives the critical modified factor λ_c as a function of g_e , showing that at critical ϕ_p ,

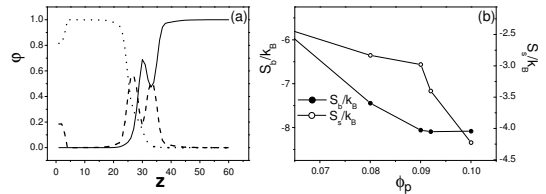


FIG. 3: (a) Lateral statistical concentration morphology of brush(dotted curve), free chains(solid curve), and particles(dashed curve) for $\phi_p = 0.1$. (b) Entropies of brushes (S_b) and solvent (S_s) vs ϕ_p .

the effective shear modulus first increases with increasing g_e and then slightly decreases at large g_e . For small g_e , the shear modulus increases with g_e , indicating that the correlation between cylinders is enhanced due to the decrease of d_c . In contrast, for large g_e , the minimum spacing between cylinders keeps almost unchanged, but the embedding depth ϵ_c becomes larger than the cylinder radius so that the grafted chains can cross the narrow gap between cylinders and fill the upper space. Thus, the grafted chains are slightly released, which accounts for small decrease of λ_c at large $g_e (> 0.5)$.

The formed first-layer colloidal crystal may serve as a template for next-layer structural formation, and thus provides a possible route to the fabrication of multi-layer microstructures. We find from Fig. 1(f) that the second layer is well arranged, based on the already deposited layer. However, the morphology selection of second-layer colloidal dispersions will be affected by the entropic effect of solvent polymers. By calculating the z -direction averaged density profiles of brushes, free chains, and particles for the case of Fig.1(f), Fig. 3(a) clearly shows that more solvent chains will fill the space between the first layer and the second layer of cylinders. Therefore, the second-layer cylinder structure is selected to alternately arrange with the first layer for increasing the configurational entropy of confined solvent chains. In fact, the alternating arrangement of cylinders in Fig. 1(g) further supports our viewpoint on controlled layer-by-layer growth driven entropically by polymer solvent. Figure 3(b) gives the entropies of brush and solvent as a function of ϕ_p . We find that when ϕ_p takes the range $0.09 \sim 0.10$ corresponding to the forming process of second-layer structure, the brush entropy retains almost unchanged, while the solvent entropy sharply declines, meaning that the second-layer colloidal assembly is out of brush effects, instead the solvent entropy dominates the final equilibrium dispersion of the second-layer particles.

Finally, Fig.4 shows the entropy of brushes and the root-mean-square fluctuation Δ of statistical brush height h [24] as a function of g_e for $\phi_p = 0.06$ and 0.1 . We see that the brush entropy decreases with an increase of g_e , but the height fluctuation due to brush deformation increases with g_e . Correspondingly, the particle distribu-

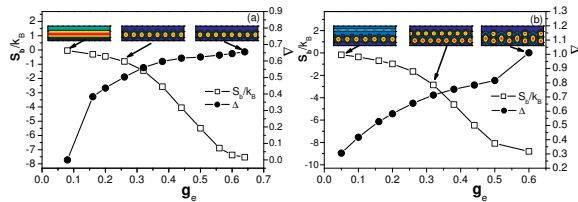


FIG. 4: The brush entropy S_b and the modulated fluctuation Δ of brush height vs g_e . (a) $\phi_p = 0.06$. (b) $\phi_p = 0.1$.

tions in the inset of Fig.4 signify the formation of cylinder structures with varying g_e . Figure 4(a) shows that for small g_e , the deposition of particles did not deform brushes which therefore do not react with the dispersion of particles. On the other hand, the relatively large range of the parameter g_e can stabilize the one-layer cylinder structures due to strongly entropic restoring forces of brushes. In contrast, Fig. 4(b) shows that a small range of g_e may retain the two-layer cylinder structures. When g_e is small, there are not enough particles deposited onto the top of brushes, leading to one-layer structure. As g_e is relatively large, the two-layer structure is destroyed, instead the alternating structure of one- and bi-layer cylinders appears, because the entropy restoring force of solvent chains is weaker than that of brushes, and may not completely offset the settling energy of particles if the

second layer is formed. It is actually interesting that the brushes have large entropic restoring forces which easily stabilize colloidal dispersions. For example, depending on the colloidal weight and volume fraction, brushes can adjust the number of cylinders formed, in contrast to colloidal crystallization in non-adsorbing polymer solvent.

In summary, we have demonstrated that under suitable density and depositing force of particles, colloidal particles can be sorted into alternating arrays of cylinders by use of grafted substrates. The colloidal dispersions are dominated by the requirement of minimizing combinational contribution of depositing potential of particles and entropic restoring force of the deformed brushes. With an increase of colloidal additions, controlled layer-by-layer growth is driven by entropic effects of solvent chains. The advantage of the present approach is that control over arrangement of colloids did not rely on other patterned [2] and phase-separated copolymer [3] templates but was achievable via a polymer-grafted substrate which is easily manufactured. The approach that under sedimentation, polymer entropic restoring force drives ordered structure formation, will offer a simple and powerful alternative for producing 2D and even 3D structures, and may open up an unexplored route for engineering highly ordered structures from colloidal building blocks.

This work was supported by the National Natural Science Foundation of China under Grant Nos. 10334020, 10021001, and 20490220.

-
- [1] G. W. Whitesides and M. Boncheva, *Proc. Natl. Acad. Sci.* **99**, 4769 (2002); J. Zhu et al., *Nature* **387**, 883(1997).
- [2] A. V. Blaaderen, R. Ruel, and P. Wiltzius, *Nature* **385**, 321(1997); K. Lin et al., *Phys. Rev. Lett.* **85**, 1770(2000); Y. Yin et al., *J. Am. Chem. Soc.* **123**, 8718(2001).
- [3] W. A. Lopes and H. M. Jaeger, *Nature* **414**, 735(2001); M. J. Misner et al., *Adv. Mater.* **15**, 221(2003); M. R. Bockstaller et al., *J. Am. Chem. Soc.* **125**, 5276 (2003).
- [4] L. Ramos et al, *Science* **286**, 2325(1999).
- [5] Z. Liu et al., *Nano. Lett.* **2**, 219(2002).
- [6] J. U. Kim and B. O'Shaughnessy, *Phys. Rev. Lett.* **89**, 238301 (2002).
- [7] Y. Lin et al., *Science* **299**, 226(2003).
- [8] H. Wickman and J.N. Korley, *Nature* **393**, 445(1998).
- [9] K. Chen and Y. Ma, *J. Phys. Chem. B* **109**, 17617(2005); C. Ren and Y. Ma, *J. Am. Chem. Soc.* **128**, 2733(2006).
- [10] S. T. Milner, *Science* **251**, 905(1991); J. Satulovsky, M. A. Carignano, and I. Szleifer, *Proc. Natl. Acad. Sci.* **97**, 9037 (2000).
- [11] M. Biesalski and J. Ruhe, *Macromolecules* **32**, 2309(1999); J. Habicht, M. Schmidt, J. Ruhe, and D. Johannsmann, *Langmuir* **15**, 2460(1999).
- [12] P. G. Ferreira, A. Ajdari and L. Leibler, *Macromolecules* **31**, 3994 (1998).
- [13] R. B. Thompson et al., *Science* **292**, 2469 (2001); *Macromolecules* **35**, 1060 (2002).
- [14] M. W. Matsen and M. Schick, *Phys. Rev. Lett.* **72**, 2660(1994); D. Petera and M. Muthukumar, *J. Chem. Phys.* **109**, 5101(1998); F. Schmid, *J. Phys.:Condens. Matter* **10**, 8105 (1998); M. W. Matsen and F. S. Bates, *J. Chem. Phys.* **106**, 2436(1997); P. Maniadi et al., *Phys. Rev. E* **69**, 031801(2004); M. Muller, *Phys. Rev. E* **65**, 030802(2002); T. Geisinger, M. Muller, and K. Binder, *J. Chem. Phys.* **111**, 5241(1999).
- [15] F. Drolet and G. H. Fredrickson, *Phys. Rev. Lett.* **83**, 4317 (1999); *Macromolecules* **34**, 5317 (2001).
- [16] P. Tarazona, *Mol. Phys.* **52**, 81(1984).
- [17] N. F. Carnahan and K. E. Starling, *J. Chem. Phys.* **51**, 635(1969).
- [18] The interaction of colloidal particles can be adjusted by chemically coating ligands onto the surfaces of them.
- [19] T. Biben, J. P. Hansen, and J. L. Barrat, *J. Chem. Phys.* **98**, 7330(1993); C. I. Addison, J. P. Hansen, and A. A. Louis, *ChemPhysChem* **6**, 1760(2005).
- [20] M. Holgado et al., *Langmuir* **15**, 4701(1999).
- [21] M. Trau, D. A. Saville, and I.A. Aksay, *Science* **272**, 706(1996); M. Giersig and P. Mulvaney, *J. Phys. Chem.* **97**, 6334(1993); *Langmuir* **9**, 3408(1993).
- [22] N. V. Dziomkina and G. J. Vancso, *Soft Matter* **1**, 265(2005).
- [23] Y. Bohbot-Raviv and Z. G. Wang, *Phys. Rev. Lett.* **85**, 3428(2000).
- [24] We define $\varepsilon = \max(h(x)) - \min(h(x))$, where the local

brush height $h(x) = 2 \sum_z \varphi(x, z)z / (\sum_z \varphi(x, z))$.

[25] G. H. Fredrickson et al., *Macromolecules* **25**, 2882(1992).